Equilibrium Structures of Three-Dimensional Complex Plasma Clusters Suspended in a Glass Box

Suzannah R. Wood,* Victor Land,† Jorge Carmona-Reyes, Jonathon Dallas, Lorin Matthews, and Truell Hyde‡
Center for Astrophysics, Space Physics & Engineering Research,
Baylor University, One Bear Place #97310, Waco, TX 76798
(Dated: August 5, 2010)

Experiments to study the equilibrium structure of small three-dimensional complex plasma clusters were performed inside a modified GEC reference cell. Horizontal confinement was provided by a glass box situated on the lower electrode. Single particle trajectories of dust particles were analyzed to determine the horizontal confinement. Three dimensional reconstructions were obtained using a dual CCD camera imaging technique. Finally, these structures were compared with numerical simulation from an N-body model.

I. INTRODUCTION

Complex (dusty) plasmas are found in many natural and manmade environments, and have been an interest to scientist due their unique properties. Complex plasmas can be found in natural environments like Saturn's rings, comets, and nebulae[1]. Synthetically created plasma exists in the semiconductor manufacturing, which uses plasma to etch wafers [2]. Complex plasmas have been studied under microgravity conditions[3], as well as under gravity, in both two- [4] and three-dimensional systems[5]. There have been investigations into the melting and phase transitions of this plasma in two-[6] and three-dimensions[7] [8] [9]. Complex plasma is an excellent system for studying strongly coupled systems, due to their macroscopic size, slow dynamics and transparency[10]. Confinement of these clusters was first described by O. Arp[10], where the vertical confinement forces were discussed, these included: the force of gravity, the thermophoretic force, and the ion drag force. The electric field force is mentioned to contribute to the horizontal confinement; however, this force is not investigated in depth. This study investigates the horizontal (radial) confinement force experienced by the dust cloud.

Imaging techniques have been developed to record the behavior and position of these particles within plasma. Although these techniques were often complicated, they provided quite precise particle positions in three-dimensions. One such technique is a stereoscopic in-line holography technique which uses the interference of waves to identify particle positions[5]. Another technique is a stereoscopic observation method. One scheme proposed used two cameras offset by 15°[11]. Another stereoscopic imaging approach used three cameras, where at least two cameras observe each particle[9]. Here, another dual CCD camera was used to record the equilibrium structure of three-dimensional complex plasma clusters. The goal of using this technique is to cut down on the complexity of the imaging technique, while still retaining the accuracy.

Finally, this study applies the imaging technique to the study of the equilibrium structure of three dimensional complex plasma clusters, and compares these results to N-body model.

II. EXPERIMENTAL SETUP

A. GEC rf Reference Cell

The experiments were conducted in a modified General Electronics Conference rf (GEC) Reference Cell, which is powered by a 13.56 MHz radio frequency coupled discharge[12]. This cell, whose schematic is depicted in Figure 1 contains, two 10.16 cm-diameter electrodes, separated by 2.54 cm. The top electrode is grounded and consists of a hollow cylinder to allow for Melamine-Formaldehyde dust (8.89 m) to be manually dropped into the plasma. The electrode also allows for the top CCD camera to capture the laser light reflected from the dust.

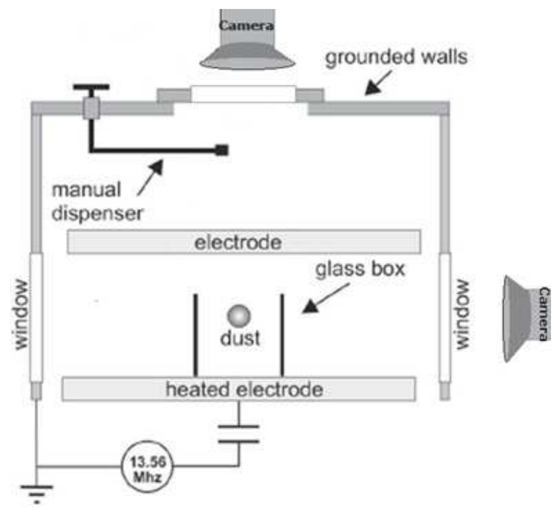

FIG. 1. A sideview cross sectional schematic of the modified GEC rf Reference Cell.[10]

* swood13@cornellcollege.edu
† Victor_Land@baylor.edu
‡ Truell_Hyde@baylor.edu

The laser used was a diode laser with a wavelength equal to 636 nm. The powered bottom electrode has the ability to be heated or cooled (experimental temperatures ranged between $16° - 66°$ C). A 22 mm x 22 mm x 20 mm glass box, with glass thickness of 2 mm, was situated on the electrode, to extend horizontal confinement of the dust particles vertically. Experimental pressures were between 13.3 and 60 Pa.

B. The Cameras

Two different sets of two CCD cameras each were used to record the experiments. These cameras were equipped for movements along all three axes, and automated movement along the axis of view. A pair of XC-HR50 Sony CCD cameras was used to record the stable structure of the cluster. The camera situated above the cell was used to record horizontal structure. The camera at the side of the cell was used to record the vertical structure. High speed CCD cameras (FAST-CAM 1024PCI) were used to record single particle trajectories. The top view camera looked down the z-axis, and captured a xy-plane, with coordinates (-y,x). This camera was equipped with the Navitar 7000 lens. The side view camera was equipped with the Infinity lens- Model K-2. This camera looked down the x-axis and captured a yz- plane, with coordinates (y,z). This coordinate notation was instrumental in three-dimensional reconstructions.

III. RADIAL CONFINEMENT

Previous experiments found a parabolic potential for confining three-dimensional dust clusters, which assumes axial symmetry [10]. Non-circular cross sectional areas were noted in photos taken by the high speed camera, as seen in Figure 2. This cross-sectional area is in disagreement with previous literature[1].

The single particles were observed to move all along the outline of the crystal cross section. Therefore three single particle trajectories were recorded to trace the potential energy well, as seen in Figure 3. These trajectories are a good tool for calculating the radial confinement force. They were observed under the conditions of 57.7 Pa and an rf signal of 7.2 W.

As seen in Figure 3, the particles' trajectories have a rounded square path. These particles experience a horizontal electric confinement force acting towards the center of rotation and an equal but opposite centrifugal force acting away from the center of rotation. The x-, y- and radial position with respect to time can seen in Figure fig:position. The particle movement in the x-direction and y-direction seem to be sinusoidal. This sinusoidal motion indicates a periodic rotation motion. Assuming a circular path of rotation, this force can be approximated by

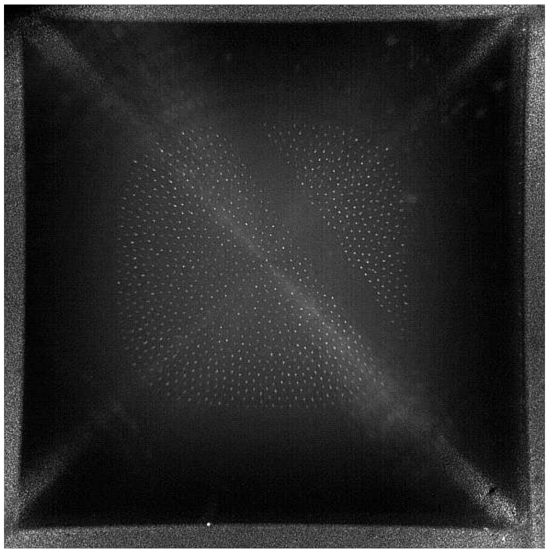

FIG. 2. The horizontal cross section of the crystal taken by the high speed CCD top-view camera recorded at 250 fps. Note that the diagonal shade is caused by the glass box. It is assumed that the structure continues through the void.

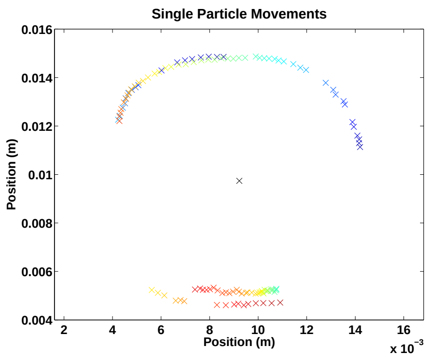

FIG. 3. Single particle trajectories particles positions by the top-view camera recorded at 60 fps. Motion in time indicated by color, where start of trajectory blue and the end of trajectory is red [see color online].

$$F = -mv^2/r \tag{1}$$

where m is the mass of the particle, v is the tangential velocity of the particle and r is the radius of rotation. Figure 5 shows the absolute value of the confinement force at different radii from the center of rotation. As seen in Figure 5, different radii result in different confinement forces. From the data collected, radius and confinement force seem to have a direct relationship as one increases so does the other. Additional trials and different approaches are needed, in order to establish whether the horizontal confinement well differs from literature. A linear force trend would imply a parabolic energy well. This trend would indicate that our confinement is in agreement with literature[10]. Although the calculations approximated the path of the dust particles to be circular, it was not, if it were the radial position in Figure 4 would be a constant value. Thus, it is reasonable to argue that the axial symmetry of the glass box used in these experiments differs from literature.

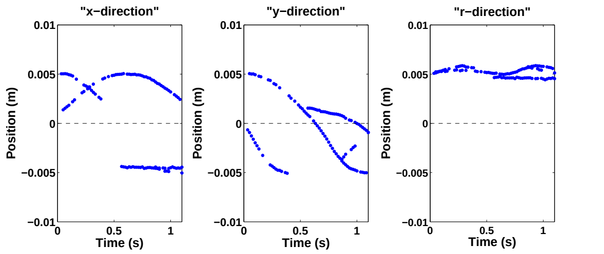

FIG. 4. Single particle trajectories particles positions by the top-view camera recorded at 60 fps, the x-, y- and radial motion is shown. The particles movement in the x- and y-direction seems to be sinusoidal.

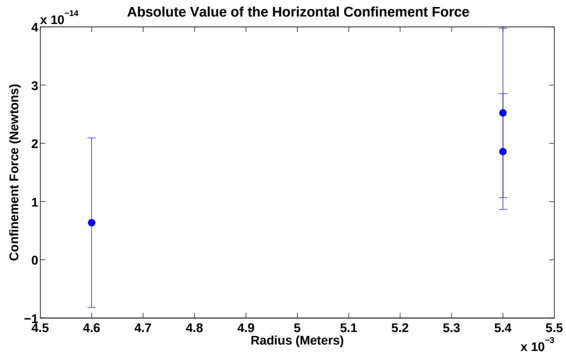

FIG. 5. Radial confinement force for different radii from the center of rotation. The points are the force, for the average velocity at that given radius. The lines are the values within one standard deviation of the point. There are only two radii because only three trajectories were recorded

IV. IMAGING TECHNIQUE - CLUSTER RECONSTRUCTION

Due to the fact that dust clusters are 3D structures, three-dimensional imaging techniques need to be employed so that the structure and dynamics of the clusters can be analyzed. Here another technique for three-dimensional imaging is described. This technique can best be described as slicing an onion, where each slice of the onion is a plane where particles lie. The camera and corresponding laser were mechanically stepped from one end of the cluster to the other with constant step-size. The step size of the camera and the laser were synced so that the focal length remained constant. The step size was 119.1 $\pm$ 0.7 μm comparable to the interparticle distance of particles within a dust cluster. A set of five frames were taken at each step, using a slave and master technique. The average position of each particle detected in the five frames per step was found to eliminate error from noise. The particle positions were then assigned a third coordinate based on the step position of step where they were recorded. This process was followed for each camera (top and side). For the top camera, frames recorded the xy-plane, where the z-axis is reconstructed based on the position of the step of the laser and camera. For the side camera, frames recorded the yz-plane, where the x-axis was reconstructed from the position of the camera and laser. The reconstructions were centered at the center of mass of the cluster. Figure 6 shows a side- and top-view reconstruction where each of the respective centers of mass is centered at the origin. As seen in Figure 6 the reconstruction is not perfect: the particles do not overlap. However they are in the same region of the graph. This is better observed in Figure 7 which displays the projection of both reconstructions onto the xy-plane.

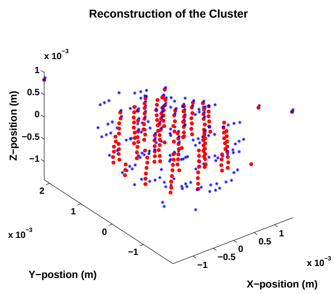

FIG. 6. Three-dimensional reconstructions of the same complex plasma cluster. The blue stars are from side view reconstruction, the red dots are from the top view reconstruction. [color online]

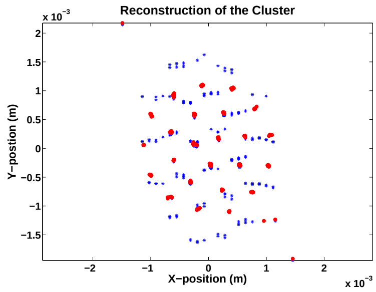

FIG. 7. Projection of cluster reconstructions onto the xy-plane The blue stars are from side view reconstruction, the red dots are from the top view reconstruction.

V. NUMERICAL MODEL

Not only was the equilibrium structure of three dimensional complex plasma investigated experimentally, numerical simulations were also run using an N-body code. The code has been used in the past to model many systems ranging from charged grains in a planetary magnetic field[13]and multiple sized grains in a dust crystal[14][15].This code uses a parabolic radial confinement, which is consist to literature[10]. It uses a force balance for vertical confinement. The horizontal confinement is provided by a parabolic potential energy well. The potential well in the code is similar to that produced by a circular depression in the electrode experimentally. To extend the horizontal confinement vertically and produce a potential well that better models the experimental conditions, the potential well in the code was multiplied by constant multiples.

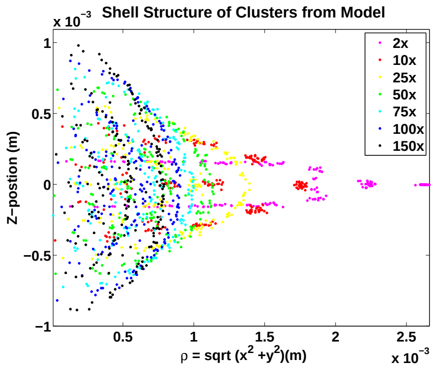

FIG. 8. This plot displays the shell structure of various multiples of the Box_Tree code. There are 200 particles in each different shell structure. The quantity ρ represents the distance from the z-axis.

Figure 8 displays the cluster structure from various multiples of the code's original parabolic confinement. The optimum confinement of this cluster is shown in Figure **??**. This amended potential well is in agreement with literature[1]. The shell structure is in good agreement with literature[16][8][9]. The cluster, displayed in Figure 9, consists of 200 particles. This cluster has four concentric spherical shells, the first shell has 6 particles, the second shell has 31 particles, the third shell has 67 particles, and the outer shell has 96 particles, these shells can be seen in Figure 10. The surface of this cluster is tiled in hexagons with connecting pentagons. This structure suggests a Yukawa interaction.[8][17]

VI. DISCUSSIONS

Although, the equilibrium structures of three-dimensional complex plasma have been analyzed and constructed before, these investigations are new for our laboratory[10] [16] [17]. The radial confinement investigations have proven to be inconclusive for finding a confinement force, yet they have still yielded useful insight into the process. The limited data available does not exclude parabolic radial confinement, although it does not concretely support this confinement. It is reasonable to conclude that the axial symmetry of the confinement does

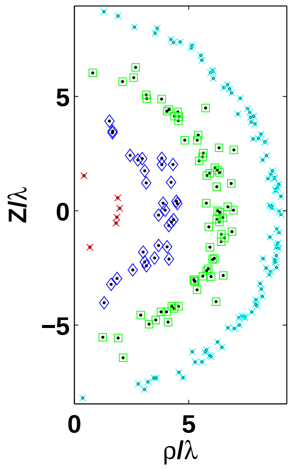

FIG. 9. The shell structure of cluster from optimum parabolic confinement, where λ is the debye length. This cluster displays a Yukawa interaction. Each shell of the four shells is a different color (See color online).

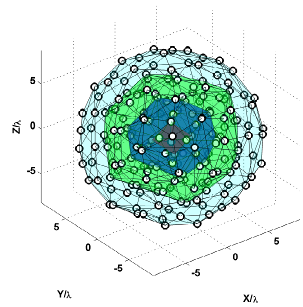

FIG. 10. Three-dimensional structure of cluster from optimum parabolic confinement, where λ is the debye length. Each shell of the four shells is a different color. This shows the topography of the shell structure. (See color online).

differ from previously confinements[10]. This conclusion is drawn from cross sectional area of the cluster see Figure 2 and from the path of the single particle trajectories see Figure 3. If a closer look is taken at Figure 2, one can notice the inward bowed nature of the glass walls, the walls are not bowed inward, this distortion is from the aberration due to the Navitar 7000 lens structure. For these conclusions to hold true, it is important that the curvature of the lens was not the cause of the distortion of the crystal or of the single particle trajectories. This being a first order approximation, the distortion was not taken into account, for a more complete investigation of the radial confinement, this defect must be taken into account.

The dual CCD camera technique has potential to be a simpler yet just as precise method for three-dimensional imaging. There are several considerations that need to be taken into account before this technique completely refined. One of the largest problems with the current method is over counting of particles. This has several causes. The laser beam sheet used to illuminate the particles is approximately 100 - 200 μm wide, where the camera and laser step size was only 119 μm. This difference leads to significant overlap between slices. To correct this issue a more accurate measure of the beam width needs to be taken into account so that slices can be adequately spaces. Also, the beam is also not a constant intensity or width; in fact, the laser beam intensity has a Gaussian profile, where the intensity of the beam is greatest in the center and a divergent. Differences in beam width and need to be taken into account in the particle detection algorithm. Also, an algorithm for excluding outlining particles needs to be developed based on the average interparticle distance, to eliminate particles that are not part of the cloud or noise picked up in particle detection. This algorithm would also identify same particles by looking for multiple particles within a percentage of the interparticle average distance, average the position of these particles and insert a single particle at this new location. Another considea that must be taken into account in the lab is that the mounting of our cameras. In the HIDPL lab, the normal top-view view can be mounted in four directions with means the xy-plane can be rotated in four directions. The direction of the top-view must be consistent. Further considerations for the HIDPL include the fact the cameras field of view are not strictly perpendicular, causing the two camera axes to not overlap directly but instead have an angle θ between them. This angle needs to be taken into account in the reconstruction algorithm.

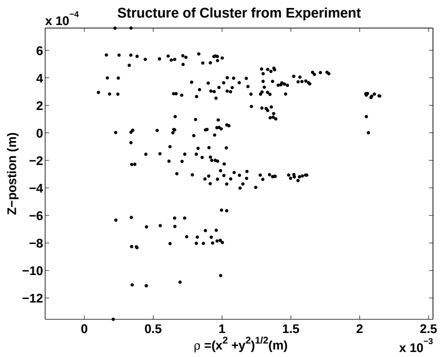

FIG. 11. The shell structure of cluster from experimental reconstruction. This cluster does not display a Yukawa interaction.(See color online).

Figure 11 and Figure 9 compare the shell structure of the experimental cluster and the model structure respectively. The model cluster displays a Yukawa interaction due to the concentric shells. The experimental cluster does not have this shell order, and therefore it is must likely not a Yukawa ball. Although, this cluster does not have a Yukawa interaction, the vertical alignment in chains (not pictured, but observed) as well as the shell structure, shown in Figure 11 is constant with clusters influences by ion wake fields described by Kroll[5]. To further investigate this phenomenon, it would be useful to investigate the effect of the ion wake field in the N-Body simulations.

VII. CONCLUSIONS AND OUTLOOK

Here, a new technique for imaging three-dimensional clusters is proposed, though not refined improvements have been proposed to improve this method, including error eliminating algorithms and considerations to the physical set up have been noted. Though this is a first order approximation study for the potential well and the horizontal confinement force on Yukawa balls and complex three-dimensional plasma cluster and not all the data was conclusive, this investiagation led to a solid method for determining the horizontal confinement force. When more single particle trajectories are observed, this model will be applied to find the horizontal confinement force and the confining potential energy well. Although, the equilibrium structure observed experiemently is most likely not a Yukawa ball, it was highly structured. This structure included the vertical alignment in the form of extended chains. The Yukawa interaction however, is observed in the model. To gain a better understand of experimental results and see if the ion wake effect has a significant effect on the structure of the experimental clusters, the effect of ion wake fields needs to be added the numerical simulation. This paper lays the foundations for further three-dimensional complex plasma clusters investigations at the HIDPL laboratories.

ACKNOWLEDGMENTS

We would like to acknowledge the National Science Foundation for funding this work through the NSF REU Summer 2010 Grant. We would also like to thank all the members of CASPER and HIDPL for simulating discussion and advice, especially Mike Cook and Jimmy Schmoke for their extensive work on the experimental apparatus.

[1] H. Baumgartner, D. Block, and M. Bonitz, Contributions to Plasma Phys. **49**, 4-5, 281-302 (2009).
[2] R.L. Merlino and J.A. Goree, Phys. Today **57**, 7, 32-39, (2004).
[3] A.P. Naefedov, *et. al.*, New J. Phys., **5**, 33 (2003).

[4] J.Böing, A. Filinov, P. Ludwig, H. baumgartner, M. Bonitz, Yu.E. Lozovik, Phys. Rev. Lett. **11**,113401 (2008).
[5] M. Kroll, J. Schablinski, D. Block, A. Piel, Phys. Plasmas **17**, 013702 (2010).
[6] V. Nosenko, S.K. Zhdanov, A.V. Ivlev, C.A. Knapek and G.E. Morfill, Phys. Rev. Lett. **103** 015001 (2009).
[7] S.W.S. Apolinario and F.M. Peeters, Phys. Rev. E **76**, 031107(2007).
[8] D. Block S. Käding, A. Melzer, A. Piel, H. Baumgartner, and M. Bonitz, Phys. Plamsa **15**, 040701 (2008).
[9] S. Käding, D. Block, A. Melzer, A. Piel, H. Kählert, P. Ludwig, and M. Bonitz, Phys. Plasma **15**, 073710 (2008).
[10] O. Arp, D. Block, M. Klindworth, and A. Piel, Phys. Plasmas **12**,122102 (2005).
[11] S. Käding and Andre Melzer, Phys. Plasmas **13**, 090701 (2006).
[12] P. J. Hargis, *et. al.*, Rev. Sci. Instrum. **65**, 1, 140-154 (1994).
[13] L.S. Matthews and T.W. Hyde, Advances in Space Research **33**, 2292-2297 (2003).
[14] L.S. Matthews, K. Qiao, and T.W. Hyde, Advances in Space Research **38**, 2564-2570 (2006).
[15] B. Smith, T. Hyde, L. Matthews, J. Reay, M. Cook, and J. Schmoke, Advances in Space Research **41**, 1510-1513, (2008).
[16] M. Bonitz, D. Block, O. Arp, V. Golubnychiy, H. Baumgartner, P. Ludwig, A. Piel, and A. Filinov, Phy. Rev. Lett. **96**, 075001 (2006).
[17] A. Piel, Plasma and Fusion Research **4**, 013 (2009).